Journal of Diabetes Science and Technology
2018, Vol. 12(6) 1169–1177

DOI: 10.1177/1932296818798347
journals.sagepub.com/home/dst
SAGE

Noninvasive Monitoring of Blood Glucose Using Color-Coded Photoplethysmographic Images of the Illuminated Fingertip Within the Visible and Near-Infrared Range: Opportunities and Questions

Thorsten Vahlsing, Dipl-Ing[1,2], Sven Delbeck, MSc[3], Steffen Leonhardt, PhD, MD[2], and H. Michael Heise, PhD[3]

Abstract

Noninvasive blood glucose assays have been promised for many years and various molecular spectroscopy-based methods of skin are candidates for achieving this goal. Due to the small spectral signatures of the glucose used for direct physical detection, moreover hidden among a largely variable background, broad spectral intervals are usually required to provide the mandatory analytical selectivity, but no such device has so far reached the accuracy that is required for self-monitoring of blood glucose (SMBG). A recently presented device as described in this journal, based on photoplethysmographic fingertip images for measuring glucose in a nonspecific indirect manner, is especially evaluated for providing reliable blood glucose concentration predictions.

Keywords

color sensing, noninvasive glucose sensing, plethysmographic skin imaging, skin tissue spectroscopy, visible/near-infrared spectroscopy

Diabetes mellitus is a wide spread disease with significantly rising numbers so that health care budgets will see worldwide a greater part being spent for people with diabetes in the future. There is need for an early diagnosis of this disease as the risk exists for the development of micro- and macrovascular complications with final appearance of blindness, kidney failure, heart disease, and nerve damage. Tight glycemic control has been proved for reducing the risk of these complications in people with either type 1 or type 2 *diabetes mellitus*. One of the recommended practices to achieve this objective is by self-monitoring of blood glucose (SMBG) levels with skin puncture for blood sampling. Self-management plans for glycemic control usually require a measurement of (finger) capillary blood, as performed by widely used blood glucose test systems;[1] see report on exemplary devices that were tested for their analytical performance.[2] Alternate testing sites have also been suggested, but interferences from either intrinsic (eg, physiology related like different/delayed glucose concentration changes depending on the measurement site)[3] or extrinsic effects (such as environment related like a sudden temperature change) may lead to a biased value with deviations from the true blood glucose concentration.

Advancements in diabetes technology can nowadays offer different sensor devices also for continuous glucose monitoring (CGM), which are still minimal-invasive approaches for reaching the ambitious and challenging goal of normoglycemia in such people. For devices without direct access to capillary blood, as for needle-type CGM sensors that monitor the interstitial glucose level, effects from calibration to the inaccessible physiological skin site require additional attention.[4] Another category of devices will aim at noninvasive pain-free technologies, for example, based on optical techniques. So far, even for this category of devices, invasive blood measurements may be required for the device calibration stage.

[1]Bundesanstalt für Materialforschung und -prüfung (BAM), Acoustic and Electromagnetic Methods, Berlin, Germany
[2]Chair for Medical Information Technology, Helmholtz Institute for Biomedical Engineering, RWTH Aachen University, Aachen, Germany
[3]Interdisciplinary Center for Life Sciences, South-Westphalia University of Applied Sciences, Iserlohn, Germany

Corresponding Author:
H. Michael Heise, PhD, Interdisciplinary Center for Life Sciences, South-Westphalia University of Applied Sciences, Frauenstuhlweg 31, D-58644 Iserlohn, Germany.
Email: heise.h@fh-swf.de

Progress in available and emerging glucose monitoring techniques and devices can be found in a recent report, downloadable from the website of the Institute of Health Economics (IHE);[5] the authors cover the whole range of methods including CGM devices (for further reviews, see Cappon et al[6] and Kim et al[7]) and noninvasive technologies, which have also been reviewed by other authors.[8,9] In this issue of the *Journal of Diabetes Science and Technology* a device called TensorTip Combo Glucometer by Cnoga Medical Ltd is introduced by Segman,[10] as an approach for noninvasive monitoring from color image sensor data that does not "focus on the glucose molecule", but on "on real-time color photography related to glucose concentrations in the capillary tissue" as a statement from him. In contrast to this, a concentration related chemical or physical property of the glucose molecule is otherwise an essential part of the measurement chain of most analytical methods or sensors suggested. The understanding of these properties and their interaction with intrinsic and extrinsic effects, as well as the calibration process is an important basis to identify and evaluate potential interference risks and to depend less on chance findings of potentially harmful impacts.

In this article, Segman's approach to noninvasive glucose concentration estimation will be analyzed also in view of the glucose optical absorption features, which have been the basis of most noninvasive assays published so far. Our comments are based on the available literature and the handbook of the TensorTip device.[10-13] Segman's article describes an initial stage of development, as mentioned under his general notes.[10] For a more recent study,[11] improvement over the described stage is claimed. It seems reasonable to conclude that the quoted incorporation of the time of measurement as feature for glucose prediction is part of this advancement.

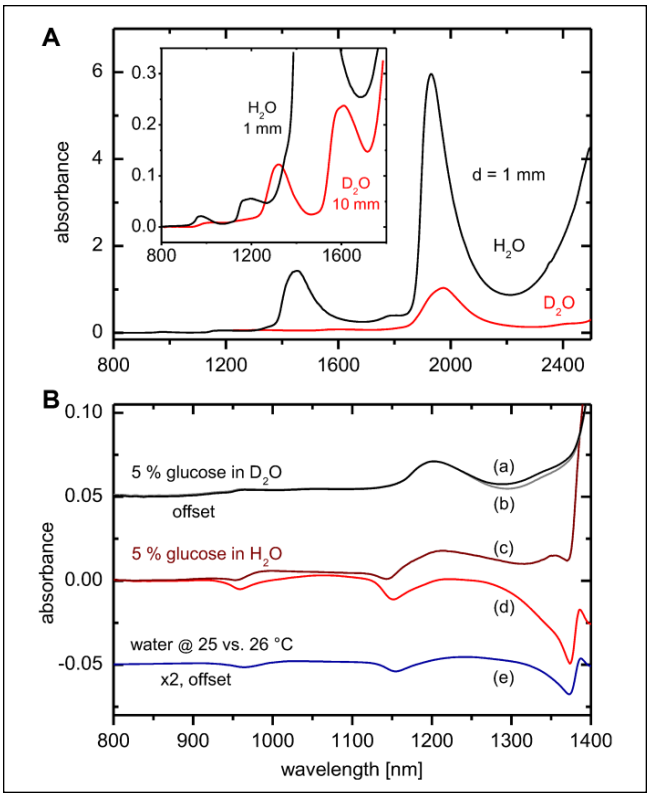

Figure 1. (A) Absorption spectra of H_2O and D_2O at various optical pathlengths and 25°C within the VIS/NIR spectral range. (B) Glucose absorption spectra at 25°C with D_2O as solvent with compensation of displaced deuterated water (a); solution spectrum measured versus a solvent filled cell (b). Glucose spectrum measured in normal water with compensation of displaced water (c) and as measured versus a solvent filled cell (d). Temperature effect on the water absorption spectrum is shown with trace (e). Water displacement factors were calculated by using solution density data from Haynes.[15]

Optical Signatures of Glucose

There are various strategies, which make use of optical signatures of glucose, which must certainly differ from those of other skin and body fluid components to reach the selectivity for quantification, despite of some existing cross-sensitivities. Approaches with molecular optical spectroscopy, either near- and mid-infrared or Raman spectroscopy, have been successfully implemented for clinical chemistry assays for blood components, in particular for glucose. The short-wave near-infrared (SW-NIR) range including some overlap to the visible red offers best opportunities due to the therapeutic window with deepest penetration depth into skin tissue, but suffers from a reduced selectivity due to overlap of component chromophore absorption bands.

Several noninvasive assays presented in the past rely on optical parameters of glucose within the VIS/NIR spectral range, which influence absorption, but also radiation scattering within the probed skin tissue. This spectral interval has also been chosen for the TensorTip device. As water is the main constituent of tissue, the absorption spectrum and its temperature and solute dependencies are of great importance, which has its origin in drastic induced changes of the hydrogen-bonded network of the water molecules, which can be probed by absorption spectroscopy. For separating these effects from pure glucose absorptivities, deuterated water (D_2O) is introduced. In Figure 1A, absorbance spectra of water samples of 1 mm thickness in comparison to the deuterated water isotope are presented, where the overtone and combination bands have been significantly shifted to longer wavelengths due to the mass effect on the molecular vibration frequencies and away from the glucose band of interest. In Figure 1B, quantitative absorption data is presented for glucose, either in (and hidden by) normal water or within D_2O. For the latter solvent, the solute and temperature effects on the normal water spectrum have been eliminated. The spectra have been recorded versus a solvent filled cell and are shown with additional compensation of the displaced water, respectively. As obvious from the figure, the displacement effect from D_2O is much reduced compared with the

normal isotope, the spectrum of which contains also the interaction of the solute molecules with the water hydrogen network. Another known effect is from temperature changes, which is similar to the induced spectral solvent effect. The values of the glucose absorption coefficients, as measured in D_2O can be favorably compared with spectral data published by Kohl et al.[14] Figure 1 also shows the magnitude of intrinsic glucose features and those signatures, which can be also induced by other solutes found in body fluids or temperature changes.

TensorTip Combo Glucometer Device Description and Discussion

The optical system of the portable device contains several light emitting diodes (LED) for fingertip transillumination and a color image sensor for detection of photons from the probed skin tissue. The optical geometry is similar to the setup for side-scattered finger-photoplethysmography as published recently by Yamakoshi et al.[16]

For illustrating the basics of optical VIS/NIR technologies for noninvasive monitoring of tissue chromophores besides water and glucose, we compiled further relevant spectral intensity and absorbance data in Figure 2. Spectral data for eumelanin and pheomelanin are not given, as for the fingertips negligible absorption exists from these substances; for other skin areas these can influence the color of skin within the Vis/NIR spectral range significantly.[17] The inset in Figure 2A shows two exemplary reflection spectra of a fingertip and of forearm skin, providing information on tissue blood volume and hemoglobin oxygenation as measured by us. For Figure 2B the sum of four intensity normalized LEDs is shown with our assumption that the specified and reported LED center wavelengths were not just an example but actually implemented. Commercial LEDs emit a wider range of wavelengths (typically 20-60 nm full width at half maximum [FWHM]) within the considered spectral range[18] than found for sources such as diode lasers. If explicit spectral resolution is not a priority, the simultaneous illumination by different sets of LEDs, as realized for the TensorTip Combo device, instead of a sequential illumination, is advantageous when regarding time resolution.

Figure 2B shows absorbance data of fully and 95% oxygenized hemoglobin and water as main chromophores. The oxygenated hemoglobin amount in tissue changes in a pulsatile manner during a heartbeat due to blood volume modulations and causes detectable spectral changes. For many years, the well-known pulse oximeters make use of so-called photoplethysmography (PPG) in a skillful way,[19,20] based in part on the fact that many interfering effects (except motion artifacts) are slow enough to be negligible during a heartbeat. A common choice of LEDs for these devices is 660 nm and 940 nm. In Figure 3A, subsecond fiber-optic reflection measurements are presented, illustrating the pulsatile spectra of a fingertip. In Figure 3B, the average skin spectrum is given in

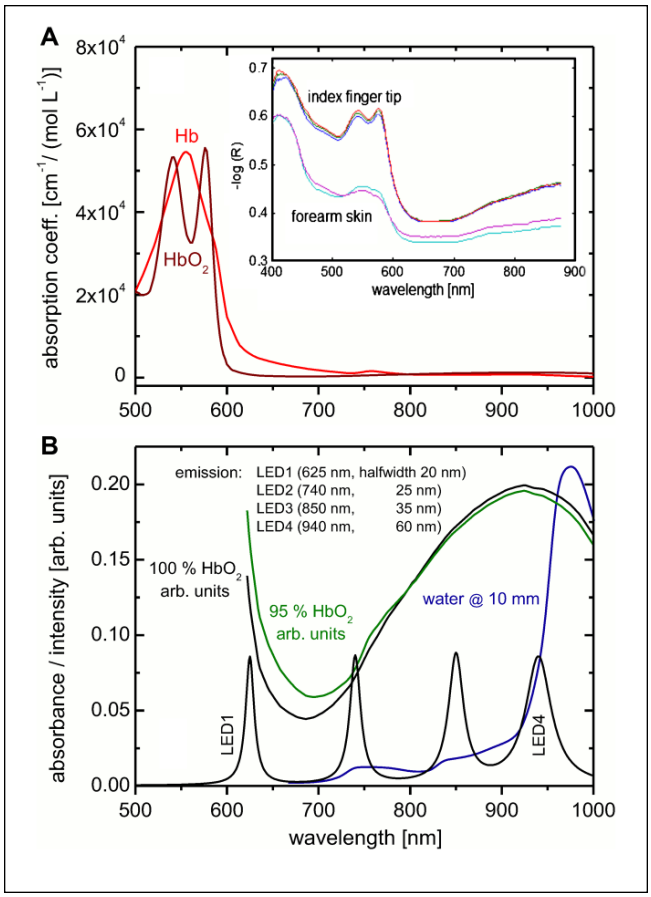

Figure 2. (A) Absorptivity data for oxy- and deoxy-hemoglobin (downloaded from https://omlc.org/spectra/hemoglobin/); the inset shows two diffuse reflection spectra of fingertip and forearm skin as measured with a fiber optic probe. (B) Spectra of hemoglobin at different oxygenation rates; included is the absorbance spectrum of water at 10 mm pathlength. Also shown is the illumination irradiance (intensity normalized) for four LEDs with indicated halfwidths from Hamamatsu Catalog[18] at selected center wavelengths, as mentioned by Segman.[10]

addition to the spectral amplitudes, as obtained from Fourier analysis of the individual wavelengths at heartbeat frequency. The inset in Figure 3B, shows part of the frequency power spectrum of the equidistantly sampled time series measurement at 580 nm with maximum Fourier coefficient at the fundamental heartbeat frequency.

Unfortunately, very little information is provided about the digital camera of the TensorTip. As Segman states, it uses a real-time color image sensor, which allows one to analyze tissue pigmentation over spatial-temporal-color domain. Further information given is on sensor sensitivity to be within 380 to 1000 nm.

Regarding the spectral characteristics of the image sensor, the article mentions a red, green and blue color plane. Conventional camera sensors use patterned color filter arrays (CFA) based on dyes and pigments over otherwise identical silicone photodiodes[21] with some transparency in the infrared,

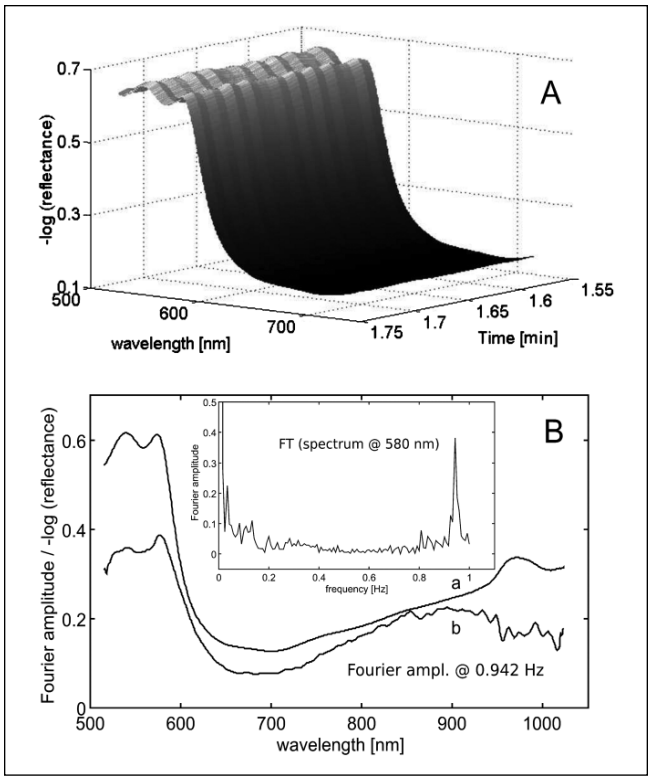

Figure 3. (A) Subsecond recording of fingertip diffuse reflection spectra using an integrating sphere. (B) Average spectrum including the scaled pulsatile spectrum at heartbeat frequency as obtained from Fourier analysis of the wavelength-dependent time series vectors; shown as inset is the power spectrum of the time series data at 580 nm wavelength up to the fundamental frequency of the transformed PPG waveform.

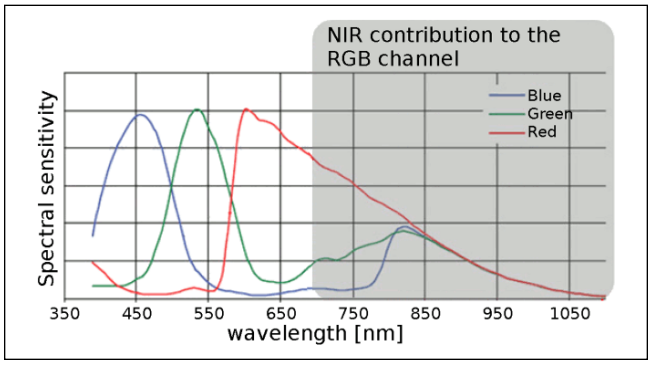

Figure 4. Spectral sensitivity of a camera sensor with Color Filter Array (CFA) modified from Park and Kang,[23] original image by C. Park and M. G. Kang, licensed under CC-BY (http://creativecommons.org/licenses/by/4.0/).

as shown in Figure 4. For digital (off-the-shelf) cameras, the resulting infrared sensitivity would cause color degradation, so it is usually blocked by a single, shared IR cut-off filter. Without such filter, a common image sensor can produce useful signals (in a technical sense, outside the domain of human vision) in all channels, although the illumination by discrete LEDs is only marginal green, red and near-infrared (see also Figure 2B). The pattern of colors in the CFA can be arranged in several ways, for example, as Bayer,[21,22] multispectral,[23] or sparse with panchromatic pixels.[24] A less common technology is the vertically stacked sensor that does not require a separate CFA.[22] In principle, also a completely custom pattern with custom filter dyes is technically possible, but may be economically infeasible for low order volumes. The spectral color response is the integral of the product of the spectral distribution of the illuminant (ie, LED at certain current value), the spectral transmittance of the finger under the experimental geometry conditions and the respective camera sensor color filter function over all wavelengths within the detector spectral sensitivity.

The boundary conditions, as mainly introduced by the requirements from the predominant markets for integrated image sensors, we suppose may explain why Segman talks about the red, green, and blue color plane on the image side. For the TensorTip MTX device, which is given as reference for the hardware description, it is stated that the sensor array uses 12 bit resolution per channel;[13] however, resolution, frame rate, and spectral sensitivity are not specified, which impedes an analysis what physiological effects could be detected at all.

First, an estimate of the impact of a glucose concentration change within the spectral range presumed for the TensorTip Glucometer is presented. Based on our spectral data of aqueous glucose for 10 mm pathlength (Figure 1B), an absorbance signal change of 25 μA.U. (micro absorbance units) within the spectral interval between 950 and 990 nm is equivalent to a glucose concentration change of 1 mmol/l. This band is the most significant spectral contribution of glucose with overlap to the 940 nm LED (Figure 2B). However, this is for an integral water measurement, with the consequence that an absolute determination would require a digital system with a change of 1 bit in a 14 bit representation for distinguishing differences of 1 mmol/l in signal intensity, which clearly shows the advantages of differential measurements if feasible.

Such estimates have been supported by simulations based on experimental tissue, water and glucose data, which have been carried out by Qu and Wilson for wavelengths of 800 and 960 nm.[25] They used a Monte Carlo simulation of the "photon random walk" based on wavelength-dependent absorption and scattering coefficients. The difficulty of obtaining accurate analytical results could be summarized by stating the optical equivalence for a change of 1 mmol/l glucose concentration, considering just water content, temperature and protein concentration, as estimated to be +0.2%, –0.1°C, and +0.1%, respectively. A by a factor of seven more sensitive temperature cross-sensitivity could be experimentally verified by us (Figure 1B), which is important also in view of the existing temperature gradients in skin. The variation of other chromophores such as oxy- and deoxyhemoglobin had not even been taken into account (blood volume change due to contact pressure or temperature stimulus,

different hematocrit values), which can have additional influences on the photometry. Similar simulations have been published by Kohl et al,[14] who presented simulated and experimental data based on light transport in a tissue phantom for the interval of 650 to 1050 nm.

In case, the pulsatile component is exploited for glucose concentration estimate, a further signal decrease of two orders of magnitude needs consideration (we noticed a factor of about 40 for our fingertip measurements with absorption bands below 600 nm; see Figure 3A). If the spectral interval around 940 nm again is considered with diffuse reflection, a blood volume change of 5% provides a pulsatile signal difference of approximately 20 μA.U. (downscaled data taken from Monte Carlo simulation in Petrov et al[17] with blood volume changes from 35 to 70 %). Another confounding parameter is hemoglobin oxygenation, where a decrease from 100% to 95% leads to an additional signal change of 5 μA.U. (see also data in Figure 2B). Beyond that, any disturbance, for example, of the pathlength through water/tissue or temperature variations, which are especially pronounced where the solvent (water) has own spectral absorption bands, would require compensation. This might give a coarse idea, why direct optical measurement of glucose with common and thus affordable detector technology based on silicon diodes (photosensitive below about 1100 nm)[23] has not achieved the required accuracy for glucose self-monitoring and why the TensorTip device approach does not try to "focus on the glucose molecule" as assured by Segman. On the other hand, Segman does not really clarify what phenomenon the device is exploiting or where to look for a (physiological) relationship between real-time color imaging and blood glucose concentration. The term "tint" is not helpful information to elucidate the measurement principle.

Discussion Based on Competing Technology

In part, integral tissue measurements have been presented, where the vascular compartment is only a fraction of the probed tissue volume. If PPG technology with information on the arterial vascular space could be implemented with a stable and high enough signal-to-noise ratio, as routinely nowadays used in pulse oximetry, also blood glucose concentration could be analyzed by using optical difference spectroscopy (see also Figure 3).

This idea has been taken up by several research groups. However, the complexity and variations of the waveform can be problematic. As described by Elgendi,[26] the main PPG waveform reflects the cardiac synchronous volume changes of arteries and arterioles as caused by the rhythmic blood pressure changes. However, there is also evidence that the PPG waveforms are also influenced from the dermal capillary density due to pressure variations from the larger blood vessels.[27,28] Lower frequency components are usually superimposed, which can be attributed to respiration, vasomotion, sympathetic nervous system activity, and thermoregulation. Various physiological and pharmacological factors exist, which influence the systolic amplitude owing, for example, to poor finger perfusion, dysrhythmia, and others.[26]

To round up the discussion of physiological parameters that are detectable in general by SW-NIR measurements, it is evident that hemoglobin chromophores in both redox states and melanin are dominating all skin-color contributions. Petrov et al[17] investigated the color of fingertip skin by Monte Carlo simulations using a multilayered skin model including their different vasculature structures within the VIS/SW-NIR spectral range. Wavelength dependent photometry based on a set of optical data for each layer with corresponding chromophore concentrations allowed a subsequent projection into color space using the digital camera specification. Certainly also pulsatile volume changes including the effect from glucose, water displacement and temperature could be simulated by such sophisticated photometric tissue model for estimating dynamic color changes.

Using color images in combination with PPG signal processing, the determination of blood concentration, oxygen saturation or the spatial distribution of melanin in the skin based on a digital imaging video has been reported in the past (see, eg, Nishidate et al[29,30]), with blood concentration based on the direct (DC) signal, while the oscillating, two orders of magnitude smaller alternating (AC) signal provides pulse information that can be related to blood flow and hemodynamics. PPG imaging of the palm of the hand at 30 frames per second, with optics for reflection measurements, has been recently applied to detect spatial distribution of blood pulsations (amplitude and phase).[27] Fingertip imaging was applied for normal conditions with skin contact and compression with significant impact on PPG amplitudes and phases.[28]

Regarding the wavelength range reported for the TensorTip, Yamakoshi et al[16] published PPG studies using a similar measurement arrangement for fingertip illumination and detection of tissue penetrated radiation with a single photodetector, coining the term of "pulse glucometry." Initial fingertip measurements were with three LEDs at 808, 1060, and 1600 nm, but a more advanced arrangement with six LEDs within the spectral range of 1550 to 1749 nm was favored, aiming at glucose-related PPG signals.

Using PPG signals from LEDs at 935, 950, and 1070 nm, relevant for glucose absorption measurements (see Figure 1), pulsatile SW-NIR signals were analyzed by Ramasahayam et al[31] using a portable device for continuous glucose monitoring. The PPG signals had been motion artefact reduced by a neural network-based on an adaptive noise cancellation filter with subsequent training of an artificial neural network (ANN) for blood glucose concentration estimation. Results from clinical trials with 100 subjects were reported with Clarke error grid analysis, while 95.4% were found within region A, which covers predictions with a maximum of 20% relative deviation to the reference values, and all remaining values found within region B.

Furthermore, based on PPG analysis, Monte-Moreno[32] contributed an approach toward noninvasive blood glucose and pressure monitoring using a pulse oximeter equipped with two LEDs, emitting at 660 and 935 nm and a self-monitoring blood glucometer. A total of 4500 measurements over one minute were recorded for 410 subjects. Features from the PPG waveform were extracted by a signal processing module after preprocessing for motion artefact elimination. Subsequently, a machine learning algorithm of either implementing ridge linear regression, a multilayer perceptron neural network, support vector machines or random forests regression was used for calibration. The method does not measure differences in time intervals or in light absorption, but exploits the effect of physiological changes on the shape of the PPG waveform and on the heart rate. The author claims that these measurements are related to the subject's hemodynamics and the blood glucose level. As physiological factors that are relevant for the method, blood viscosity and vessel compliance have been listed and claimed, while blood viscosity is mentioned to rely also on blood pressure and glucose level, altering the flux of blood in the corresponding vessels and the shape of the PPG pulse (see discussion on the PPG origin above).[32]

Other PPG waveform confounders were due to the metabolic syndrome, which causes changes in glucose and blood pressure levels as well as the general hemodynamics. Therefore, individual factors were included such as age, weight and body mass index, the relationship between diabetes and heart rate (HR), which results in HR variabilities, the emotional state as well as the blood pressure regulating respiratory frequency, which can be extracted from the low frequency PPG energy components.[32] For taking breathing and effects from the autonomic nervous system into account, low frequencies of the PPG signal had also been implemented. The device and method performance was rather poor ($R^2 < 0.64$) unless random forests regression was applied. Final results were achieved for the subject population with 10-fold cross-validation, that is, 90% of the data were used for training, leaving 10% for testing with 10 times repetition ($R^2 = 0.90$). A test for overfitting was included that consisted of training with a random permutation of the glucose reference values. As required, the system was unable to predict these meaningless reference values ($R^2_{\text{training}} = 0.017$).[32]

Calibration and Blood Glucose Prediction by the TensorTip Device Software

Whether any information beyond image sensor data and time of measurement is currently used as raw input data is not clear and is missing from his publication. After the sensor signal has been sampled and converted to digital data, a software has to calculate glucose concentrations from that data. This is done by a "proprietary mathematical NBN" (neural brain network). Its description is vague and no literature references about the used terminology or the working principle are given. In general, we would classify the technique as an associative memory and reserve the (neural) brain network term to biological systems instead of the dual use by Segman. Implementation independent properties of such networks are summarized by Kohonen.[33]

Principally, pairs of input and (desired) output vectors are learned. In the application, the memory shall "recall" the output vector if its associated input vector is presented. Such vectors are for example images. If input and output are different (eg, a person's image and his name) recalls are named heteroassociative, if they are the same the system performs autoassociative recalls. Due to the ability to recall a complete output even if the input is incomplete or distorted, autoassociative memories can be used for correction or reconstruction. Both types may be amended to show invariances to some degree, for example, in case of images to shifts, scaling, rotation or brightness of the input, which might be relevant for images of the fingertip with fingerprint surface structures and the related underlying dense capillary network (for the anatomy of microvasculature of the palmar digital skin, see Sangiorgi et al[34]). Associative memories also show the capability to interpolate and extrapolate. Information storage and retrieval by presentation of (large) sensory inputs are similar to (and derived from/inspired by) human memorization of information from the environment.

The associative network of the TensorTip device uses "feature vectors" as inputs. In general, feature vectors may simply be a concatenation of all raw pixel values of all images and all other utilized information (like the time of day of the measurement), or a processed version of that data (eg, to introduce invariances, orthogonality or a beneficial coding). An example for a simple feature extraction (in combination with a model based evaluation instead of a neural network) is given for the blood pressure monitoring by the TensorTip MTX device[13] that operates on histograms (ie, the numbers of pixels in each color channel with the same value) of the acquired images instead of the images themselves. This representation eliminates all spatial information (pixel coordinates) and makes further processing invariant to shifts and rotations (as long as the same kind of skin is viewed). The histograms are then analyzed, and features, for example, the magnitude of the maximum height/pixel count or the corresponding pixel value are calculated. These features are then processed by an algorithm to calculate the output like the pulse rate. Another method would be to use, for example, the Fourier transform. The global invariant transforms (if any implemented) and the extracted features used by the TensorTip Glucometer are not documented in any way.

The same is true for the associative memory implementation. However, the concepts indicated in this article and in previous work of Segman[35] resemble each other (vectors are "correlated", the "model is based on response of synchronized group of neurons" and other similarities shown later), thus a comparison should be appropriate. The previous work[35]

is highly interdisciplinary, but we are only concerned with the possible implementation of one of these concepts in a digital computer/digital signal processor, like the TensorTip device in this analysis.

An associative memory implementation called "HNeT" (likely an abbreviation for holographic neural technology) that is cited as an emulation of the functions described,[35] has been presented in articles by Sutherland.[36,37] The latter article is a superset of the preceding one, as it is more extensive and also contains new aspects not mentioned before. There is also an extended variant[38] that allows an interesting encoding of color images.[39] Our intention is to focus just on the parallels to and implication for Segman's presentation.

The basic characteristic of Sutherland's system is that it encodes features (real values) in the phase terms of complex numbers. The magnitudes can be used to indicate an individual confidence in the value or simply kept constant. The name holographic neural network is an analogy that lies "in the form of the constitutive equations and some general operating characteristics"[36] to (digital) holography, that is, the encoding of information as phase differences of light and the abstract phase of a complex number.

The network stores its training state in a so called correlation matrix (the memory). For the TensorTip it is reported that "new vectors" are "correlated" to the "basic learning set" (we will analyze the meaning of the latter below).

As demonstrated by Sutherland the statistical distribution density of the encoded phases of the feature vector elements is required to be uniform and symmetric. If the distribution of the underlying value (before phase encoding) is known, for example, due to a good physical model, a suitable encoding formula can be found, and associative memory shows a high storage capacity and an acceptable error. However, distribution estimation based on empirical data can be problematic if that data originates from measurements on a biological organism as complex as a human person. Even if a personal calibration is used to reduce the influence of individual differences, there may be extreme states with drastic influence on the measured glucose values. With the indirect and unspecified measurement principle without knowing about its physiological origin, the medical expert might not have the information to give appropriate advice to his patients about the limitations and pitfalls of the TensorTip Glucometer (see section above about possibly detectable effects). The techniques proposed by Sutherland[37] to equalize phase distribution, also have an impact on the generalization ability and may thus just exchange problems.

Even after evaluation of the terminology hints about the network, the components, as mentioned by Segman (the branches and loops), cannot be clearly identified. Taking a look at his Figure 2,[10] it stands out, that vectors may be part of multiple branches due to similar glucose values, but there seems to be only one "optimal loop." There is also a group mentioned with either an open or closed loop. The purpose of these loops might be to efficiently apply reinforcement learning, that improves stability, in case of too similar feature vectors[37] that are allowed and possible, in case of similar glucose values. But this is purely speculative, and we do have enough information on his work to further interpret the network components.

Critical Evaluation of the Calibration and Validation Design

In general a personal calibration with at least 25 prescheduled sensor measurements at a daily routine is recommended covering the entire personal concentration range over several days, as advised by Segman[10] and the device handbook.[12] Recalibration is required in cases where the glucose prediction is outside the calibration range, which may refer to extreme cases, or just indicate a vector too distant to other vectors in a loop. Another not further specified time for recalibration is according to an internal plan of the device, which possibly depends on the daily glucose dynamics as being different for people with diabetes of type 1 and type 2 (expressed as illness severity by Segman). Further calibration updates are realized for any measurements including invasively obtained blood glucose concentration data, if not actively rejected by the user.

For studies 1 and 2, a universal/general calibration was used, collected from several ambulatory patients of the first trial. It is not clear whether all 76 patients, who later contributed to this validation study, had been taken into account for setting up the general calibration manifold. After the extensive calibration stage, only one or two measurements (in total *only* 112 paired measurements for 76 subjects!) have been provided for validation with a date of measurement unknown, compared to the last calibration testing, which is highly critical for the performance assessment of the system.

Based on the general calibration model of study 1, 77 subjects were tested in study 2, with only one validation measurement provided. If we look at the range of the invasively obtained glucose concentration values of 97-226 mg/dl with a population mean and standard deviation of 147 ± 29 mg/dl and a MARD value of 14.9% leads to a deviation of 21.9 mg/dl for the population mean value, which is not significantly reduced compared to the glucose standard deviation of the tested population. With statistical calibrations in mind, such validation results are not meaningful for a performance test of the calibration model.

For the home study (study 3) all participants had undergone the extensive personal calibration. No personal information on disease status or physical conditions is provided. If we interpret the information given by Segman for the home study, we can assume that on average 38 measurements have been carried out after personal calibration. There is no information on daily schedule of measurements, the time gap between last calibration and follow-up validation measurement and the duration of validation tests. If we assume six tests per day, the end of the measurement campaign could be after one week. If the validation stage has

been extended over a longer period (one to three months), it is to be expected that many more calibration readings, compared to the initial personal calibration, have been implemented for updating the calibration manifold. For each validation measurement an invasive blood reference test has been carried out. If the add-on device was used, this would have triggered an admission of the result to the learning set, as part of the described recalibration procedure each time. In particular, points in the C, D, and E regions of the error grid must be explained specifically, including the determining factors of these extremely dangerous scenarios for events with results in zones D and E.

For the postmarketing evaluation no information on the whole duration of the 52 measurements has been carried out. The same problem with regard to calibration update using invasive blood glucose tests exists as discussed for study 3. In principle, the calibration and validation measurements should be separated in time and most independent as possible from each other. It is plausible that this condition has not been fulfilled for the home and postmarketing studies. These scenarios are different from studies 1 and 2, where a general calibration model had been set up from patients of the first study and used for one validation test only of each individual patient.

Conclusion

We could show that a direct measurement of glucose, based on its spectral characteristics, is not possible in the short-wave near-infrared region. Thus, the TensorTip Glucometer, in its current stage of development, requires an extensive individual calibration and additional recalibration at unknown frequency. The user guide recommends a basic usage on a daily measurement schedule similar to that used for calibration.[12] There are indicators that the time of day is used as a feature for glucose prediction. No results are presented regarding the long term stability of the calibration, the ability of the device to detect if a recalibration is necessary and thereof achieved improvement. If frequent calibrations are required to achieve accuracy, this might indicate an unstable method. The impact of recalibration or a wrong time setting (eg, in case of a user that often travels between time zones), should also be reported before more comprehensive studies are started. Without a better understanding of the numerous possible physiological effects with correlations to glucose, which have been measured and used for concentration prediction, the device safety and calibration stability properties cannot be assessed, because there is too little information to design appropriate studies. The results presented in Segman[10] and Pfützner et al[11] are of low value, if basic information, for example, on the recalibration history before and during the study is missing. As recalibration is an automatically triggered process, the user might be unaware of it.

Abbreviations

ANA, artificial neural network; AU, absorbance units; CCD, charge-coupled device; CFA, color filter array; CGM, continuous glucose monitoring; CIE, International Commission on Illumination; COTS, commercially off-the-shelf; FWHM, full width at half maximum; HNet, holographic neural technology; HR, heart rate; IHE, Institute of Health Economics; LED, light emitting diode; MARD, mean absolute relative deviation; NBN, neural brain network; NIR, near-infrared; PPG, photoplethysmography; RGB, red green blue; SMBG, self-monitoring of blood glucose; SW-NIR, short-wave near-infrared; VIS, visible.

Declaration of Conflicting Interests

The author(s) declared no potential conflicts of interest with respect to the research, authorship, and/or publication of this article.

Funding

The author(s) received no financial support for the research, authorship, and/or publication of this article.

References

1. Hönes J, Müller P, Surridge N. The technology behind glucose meters: test strips. *Diabetes Technol Ther*. 2008;10(S1). doi:10.1089/dia.2008.0005.
2. Freckmann G, Baumstark A, Schmid C, Pleus S, Link M, Haug C. Evaluation of 12 blood glucose monitoring systems for self-testing: system accuracy and measurement reproducibility. *Diabetes Technol Ther*. 2014;16(2):113-122.
3. Jungheim K, Koschinsky T. Glucose monitoring at the arm: risky delays of hypoglycemia and hyperglycemia detection. *Diabetes Care*. 2002;25(6):956-960. doi:10.2337/diacare.25.6.956.
4. Acciaroli G, Vettoretti M, Facchinetti A, Sparacino G. Calibration of minimally invasive continuous glucose monitoring sensors: state-of-the-art and current perspectives. *Biosensors*. 2018;8(1):E24. doi:10.3390/bios8010024.
5. Corabian P, Chojecki D. *IHE Report: Exploratory Brief on Glucose Monitoring Technologies*. Edmonton, AB: Institute of Health Economics; 2017. Available at: https://www.ihe.ca/publications/exploratory-brief-on-glucose-monitoring-technologies.
6. Cappon G, Acciaroli G, Vettoretti M, Facchinetti A, Sparacino G. Wearable continuous glucose monitoring sensors: a revolution in diabetes treatment. *Electronics*. 2017;6(3):65. doi:10.3390/electronics6030065.
7. Kim J, Campbell AS, Wang J. Wearable non-invasive epidermal glucose sensors: a review. *Talanta*. 2018;177:163-170.
8. Lin T, Gal A, Mayzel Y, Horman K, Bahartan K. Non-invasive glucose monitoring: a review of challenges and recent advances. *Curr Trends Biomed Eng Biosci*. 2017;6(5):1-8.
9. Uwadaira Y, Ikehata A. Noninvasive blood glucose measurement. In: Bagchi D, Nair S, eds. *Nutritional and Therapeutic Interventions for Diabetes and Metabolic Syndrome*. 2nd ed. New York, NY: Elsevier; 2018:489-504.
10. Segman Y. Device and method for noninvasive glucose assessment. *J Diabetes Sci Technol*. 2018;12(6):1159-1168. doi:10.1177/1932296818763457.

11. Pfützner A, Strobl S, Demircik F, et al. Evaluation of a new non-invasive glucose monitoring device by means of standardized meal experiments [published online ahead of print February 1, 2018]. *J Diabetes Sci Technol*. doi:10.1177/1932296818758769.
12. Cnoga. *TensorTip Combo-Glucometer User Guide. Ver. 22*. November 2015. Available at: https://cnogacare.co/wp-content/uploads/2015/01/TensorTip-Glucometer-Combo-User-Manual-V22-23.11.2015.pdf. Accessed July 3, 2018.
13. Segman Y. New method for computing optical hemodynamic blood pressure. *J Clin Exp Cardiol*. 2016;7(12):1-7. doi:10.4172/2155-9880.1000492.
14. Kohl M, Essenpreis M, Cope M. The influence of glucose concentration upon the transport of light in tissue-simulating phantoms. *Phys Med Biol*. 1995;40(7):1267-1287.
15. Haynes WM. *CRC Handbook of Chemistry and Physics*. 95th ed. New York, NY: CRC Press; 2014.
16. Yamakoshi Y, Matsumura K, Yamakoshi T, et al. Side-scattered finger-photoplethysmography: experimental investigations toward practical noninvasive measurement of blood glucose. *J Biomed Opt*. 2017;22(6):67001.
17. Petrov GI, Doronin A, Whelan HT, Meglinski I, Yakovlev VV. Human tissue color as viewed in high dynamic range optical spectral transmission measurements. *Biomed Opt Exp*. 2012;3(9):2154-2161.
18. Hamamatsu Catalog. Available at: https://www.hamamatsu.com/resources/pdf/ssd/led_kled0002e.pdf. Accessed August 6, 2018.
19. Chan ED, Chan MM, Chan MM. Pulse oximetry: understanding its basic principles facilitates appreciation of its limitations. *Respir Med*. 2013;107(6):789-799.
20. De Kock P, Reynolds KJ, Tarassenko L, Moyles JTB. The effect of varying LED intensity on pulse oximeter accuracy. *J Med Eng Technol*. 1991;15(3):111-115.
21. El Gamal A, Eltoukhy H. CMOS image sensors. *IEEE Circuits Dev Mag*. 2005;21(3):6-20. doi:10.1109/MCD.2005.1438751.
22. Hubel PM, Liu J, Guttosch RJ. Spatial frequency response of color image sensors: Bayer color filters and Foveon X3. In: Proc. SPIE Vol. 5301, *Sensors and Camera Systems for Scientific, Industrial, and Digital Photography Applications* V. Bellingham (WA): International Society for Optics and Photonics; 2004.
23. Park C, Kang MG. Color restoration of RGBN multispectral filter array sensor images based on spectral decomposition. *Sensors*. 2016;16(5):719. doi:10.3390/s16050719.
24. On Semiconductor. *Application Note AND9180D, Sparse Color Filter Pattern Overview*. Rev. 3. 2018. Available at: https://www.onsemi.com/pub/Collateral/AND9180-D.PDF. Accessed August 8, 2018.
25. Qu J, Wilson BC. Monte Carlo modeling studies of the effect of physiological factors and other analytes on the determination of glucose concentration in vivo by near infrared optical absorption and scattering measurements. *J Biomed Opt*. 1997;2(3):319-325.
26. Elgendi M. On the analysis of fingertip photoplethysmogram signals. *Curr Cardiol Rev*. 2012;8(1):14-25.
27. Sidorov IS, Romashko RV, Koval VT, Giniatullin R, Kamshilin AA. Origin of infrared light modulation in reflectance-mode photoplethysmography. *PLOS ONE*. 2016;11(10):e0165413.
28. Moço AV, Stuijk S, de Haan G. New insights into the origin of remote PPG signals in visible light and infrared. *Sci Rep*. 2018;8:8501.
29. Nishidate I, Tanaka N, Kawase T, Maeda T, Yuasa T, Aizu Y, et al. Noninvasive imaging of human skin hemodynamics using a digital red-green-blue camera. *J Biomed Opt*. 2011;16(8):086012.
30. Nishidate I, Nakano K, McDuff D, Niizeki K, Aizu Y, Haneishi H. Evaluation of arterial oxygen saturation using RGB camera-based remote photoplethysmography. In: Proc. SPIE Vol. 10501, *Optical Diagnostics and Sensing XVIII: Toward Point-of-Care Diagnostics*. Bellingham (WA): International Society for Optics and Photonics; 2018.
31. Ramasahayam S, Arora L, Chowdhury SR. FPGA based smart system for non invasive blood glucose sensing using photoplethysmography and online correction of motion artifact. In: Postolache OA, et al., eds. *Sensors for Everyday Life*. Basel, Switzerland: Springer; 2017:1-21.
32. Monte-Moreno E. Non-invasive estimate of blood glucose and blood pressure from a photoplethysmograph by means of machine learning techniques. *Artif Intell Med*. 2011;53(2):127-138.
33. Kohonen T. Various aspects of memory. In: Kohonen T, ed. *Self-Organization and Associative Memory*. 3rd ed. Basel, Switzerland: Springer-Verlag; 1989:1-29.
34. Sangiorgi S, Manelli A, Congiu T, et al. Microvascularization of the human digit as studied by corrosion casting. *J Anat*. 2004;204(2):123-131.
35. Schempp W, Segman J. Analog VLSI network models, cortical linking neural network models, and quantum holographic neural technology. In: Byrnes JS, Byrnes JL, Hargreaves KA, Berry K, eds. *Wavelets and Their Applications*. Dordrecht: Kluwer; 1994:213-260.
36. Sutherland JG. A holographic model of memory, learning and expression. *Int J Neural Syst*. 1990;1(3):259-267.
37. Sutherland JG. The holographic neural method. In: Soucek B, ed. *Fuzzy, Holographic, and Parallel Intelligence*. 6th ed. New York, NY: John Wiley; 1992:7-92.
38. Khan JI. Characteristics of multidimensional holographic associative memory in retrieval with dynamically localizable attention. *IEEE Trans Neural Netw*. 1998;9(3):389-406.
39. Gopalan RP, Lee G. Indexing of image databases using untrained 4D holographic memory model. In: McKay RI, Slaney J, eds. *AI 2002, LNAI 2557*. Basel, Switzerland: Springer-Verlag; 2002: 237-248.